Scientific Report

TRANSPARENT PROCESS

EMBO reports

Type VI secretion and bacteriophage tail tubes share a common assembly pathway

Yannick R Brunet[1,2], Jérôme Hénin[1,3], Hervé Celia[1] & Eric Cascales[1,*]

Abstract

The Type VI secretion system (T6SS) is a widespread macromolecular structure that delivers protein effectors to both eukaryotic and prokaryotic recipient cells. The current model describes the T6SS as an inverted phage tail composed of a sheath-like structure wrapped around a tube assembled by stacked Hcp hexamers. Although recent progress has been made to understand T6SS sheath assembly and dynamics, there is no evidence that Hcp forms tubes *in vivo*. Here we show that Hcp interacts with TssB, a component of the T6SS sheath. Using a cysteine substitution approach, we demonstrate that Hcp hexamers assemble tubes in an ordered manner with a head-to-tail stacking that are used as a scaffold for polymerization of the TssB/C sheath-like structure. Finally, we show that VgrG but not TssB/C controls the proper assembly of the Hcp tubular structure. These results highlight the conservation in the assembly mechanisms between the T6SS and the bacteriophage tail tube/sheath.

Keywords bacteriophage; Hcp; sheath; tail tube; Type VI secretion
Subject Categories Membrane & Intracellular Transport; Microbiology, Virology & Host Pathogen Interaction
DOI 10.1002/embr.201337936 | Received 31 August 2013 | Revised 9 December 2013 | Accepted 12 December 2013 | Published online 31 January 2014
EMBO Reports (2014) 15, 315–321

Introduction

In Gram-negative bacteria, the secretion of toxin proteins is achieved by dedicated, specialized machineries called secretion systems. The Type VI secretion system (T6SS) is highly versatile as it delivers protein effectors in either eukaryotic or prokaryotic target cells [1,2]. The T6SS is composed of 13 Tss (Type six subunits) core components that assemble a macromolecular complex spanning the cell envelope [2,3]. The TssL, TssM and TssJ membrane proteins interact to form the trans-envelope apparatus [4,5]. A number of subunits are evolutionarily, structurally and mechanistically related to proteins that form the tail of contractile bacteriophages. VgrG is a composite protein, structurally related to the trimeric gp27/gp5 hub complex forming the cell-puncturing device of bacteriophage T4 [6]. The membrane of the target cell is supposed to be disrupted by the tip of the VgrG protein that acts as a syringe. Recently, a PAAR-like protein has been shown to associate with the tip of VgrG, and by recruiting effector proteins, has been proposed to translocate these proteins into the target cell [7]. The Hcp protein is structurally related to gpV, the major tail tube protein of phage λ. Hcp is an abundant protein of the T6SS that forms a ring-shaped hexamer [8–11]. While Hcp tubes have been visualized *in vitro* [12], the existence of such tubes *in vivo* has not been evidenced. In contractile bacteriophages, prior to contraction, the tail tube is surrounded by the sheath in an extended conformation [13]. Upon infection, the phage sheath undergoes an extensive structural transition leading to its contraction and propelling the tail tube towards the target cell interior [13]. Interestingly, the TssB (VipA) and TssC (VipB) proteins assemble large tubular structures extending into the cytoplasm [14,15]. The TssB/C sub-complex exhibits cogwheel-like cross-sections resembling the bacteriophage sheath [16]. Time-lapse fluorescence microscopy further showed that these structures are highly dynamic, oscillating between extended and contracted conformations [14,15,17]. Based on homology with the bacteriophage it is thought that contraction of the TssB/C tubule propels the Hcp tube towards the exterior and the target cell. In agreement with this model, a recent study has shown that contraction of the T6SS sheath is correlated with prey cell lysis [17]. However, the existence of Hcp tubes has not been demonstrated *in vivo*. The Hcp crystal structure packing suggested that Hcp hexamers may stack either in a head-to-tail [8], head-to-head [10] or tail-to-tail [11] conformation. However, while the different modes of inter-rings interactions observed for the different Hcp proteins may reflect differences during assembly, it is formally possible that these packing are crystallographic artifacts and are not physiologically relevant. Similarly, the mode of assembly of the tube protein of contractile tailed phages remains unsolved. Cryo-electron microscopy images showed that the phage tail tube is a cylinder lacking discernable surface structures [9,13]. However, the tail tubes of non-contractile phages are composed of stacked hexamers

1 Laboratoire d'Ingénierie des Systèmes Macromoléculaires, Institut de Microbiologie de la Méditerranée, CNRS – UMR 7255, Aix-Marseille University, Marseille, France
2 Department of Microbiology and Immunobiology, Harvard Medical School, Boston, MA, USA
3 Laboratoire de Biochimie Théorique, Institut de Biologie Physico-Chimique, Paris, France
*Corresponding author. Tel: +33 491 164504; Fax: +33 491 712124; E-mail: cascales@imm.cnrs.fr

© 2014 The Authors

positioned offset on each other [18]. We therefore reasoned that an *in vivo* approach might provide information on Hcp assembly. In this study, we engineered functional cysteine variants of the Hcp1 protein encoded within the enteroaggregative *Escherichia coli* (EAEC) *sci-1* T6SS gene cluster. We substituted residues at specific positions that discriminate between head-to-tail, tail-to-tail and head-to-head packing. Our results provide strong support for a model in which Hcp1 hexamers form tubular structures *in vivo*. Importantly, we further demonstrate that the Hcp1 hexamers assemble in an ordered stacked, head-to-tail, manner and that this specific assembly is a controlled process requiring other *sci-1* gene products. Finally, we also provide evidence that Hcp1 interacts with the T6SS sheath via direct contacts with the TssB1 subunit and that Hcp1 tube formation is required for sheath polymerization.

Results and Discussion

Hcp is required for T6SS sheath assembly through interaction with TssB

While the TssB and TssC subunits have been postulated to engulf the putative Hcp conduit, experimental data regarding the relationship between Hcp and the sheath-like proteins are lacking. As TssB1 and TssC1, Hcp1 mainly localizes in the cytoplasm (see further details in the Supplementary Text and Supplementary Fig S1). Using immunoprecipitation we isolated a complex between Hcp1, TssB1 and TssC1 (Fig 1A). This result is in agreement with bioinformatics analyses demonstrating that Hcp, TssB and TssC are functionally linked [19]. To gain further information, we probed pairwise interactions between Hcp1 and TssB1 and TssC1 using bacterial two-hybrid and

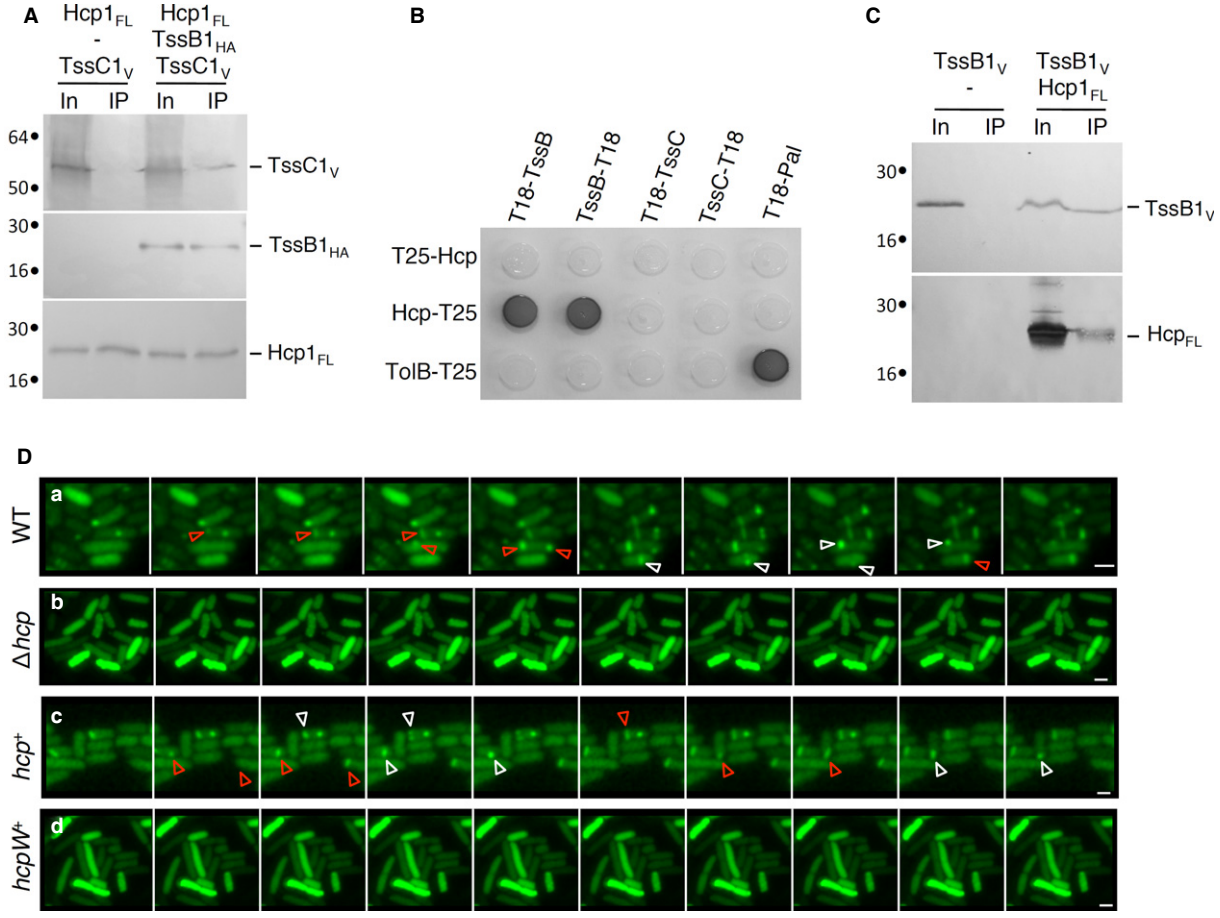

Figure 1. Hcp1 interacts with the sheath-like TssB1 subunit and is required for sheath assembly.

A–C Interaction between T6SS tube and sheath components. Co-immunoprecipitation assay are shown in (A) and (C). Solubilized extracts of *E. coli* K-12 W3110 cells producing FLAG-tagged $Hcp1_{FL}$ ($Hcp1_{FL}$), VSV-G-tagged TssC1 ($TssC1_V$) and HA-tagged TssB1 ($TssB1_{HA}$) (A) or $Hcp1_{FL}$ and VSV-G-tagged TssB1 ($TssB1_V$) (C) were subjected to immunoprecipitation with anti-FLAG-coupled beads. The input (total solubilized material, In) and the immunoprecipitated material (IP) were analyzed by 12.5%-acrylamide SDS-PAGE and proteins were immunodetected with anti-FLAG, anti-VSV-G and anti-HA monoclonal antibodies. Immunodetected proteins are indicated on the right. Molecular weight markers (in kDa) are indicated on the left. Bacterial two-hybrid assay is shown in (B). BTH101 reporter cells producing the indicated fusion were spotted on LB agar plates supplemented with X-Gal. An interaction between two fusion proteins is attested by the dark color of the colony. The TolB-T25/T18-Pal combination serves as a positive control. Non-specific interactions are ruled out using TolB-T25 or T18-Pal as negative controls.

D Time-lapse fluorescence microscopy recordings of EAEC cells producing TssB1-sfGFP. Upper panel, wild-type (WT) cells; second panel, Δ*hcp* mutant cells; third panel, Δ*hcp* mutant cells producing $Hcp1_{FL}$ (*hcp*$^+$); lower panel, Δ*hcp* mutant cells producing the S158W Hcp variant (*hcpW*$^+$). Red and white arrowheads point at extensions and contractions of the T6SS sheath-like structures, respectively. Each frame is separated by 30 sec. The scale bar represents 2 μm.

 © 2014 The Authors

co-immunoprecipitation assays (Fig 1B and C, Supplementary Text, Supplementary Fig S2). Both assays demonstrate that Hcp1 interacts specifically with TssB1, not with TssC1. Specificity experiments between the two T6SS encoded within the EAEC genome showed that Hcp1 does not interact with TssB2. Similarly, although Hcp2 interacts with TssB2, no interaction was detected between Hcp2 and TssB1 (Supplementary Text, Supplementary Fig S2). This set of data supports a model in which Hcp is wrapped by the TssB/C subunits as the bacteriophage tail tube is wrapped by the tail sheath. We next asked whether Hcp1 is required for assembly of the T6SS sheath structure. Several recent reports demonstrated that the TssB protein fused to the superfolder green fluorescent protein (sfGFP) assembles cytosolic tubular structures oscillating between extended and contracted conformations [14,15,17]. We engineered a plasmid-borne TssB1-sfGFP fusion. As previously described [20,21], this fusion protein behaves similarly to the previously described TssB-sfGFP proteins: (i) it assembles 1-3 cytoplasmic sheaths per cell, and (ii) the sheath structures oscillate between extended and contracted conformations with dynamics occurring in tens of seconds (Fig 1D, WT). These structures are not visible in a strain deleted of the *hcp1* gene, leaving a diffuse fluorescence within the cytoplasm (Fig 1D, *Δhcp*). This diffuse fluorescence phenotype was complemented by the expression of a WT *hcp1* allele from a plasmid (Fig 1D, hcp^+). The data suggest that Hcp is required for proper assembly of the T6SS sheath and that the TssB/C proteins build the sheath using the Hcp tube as a scaffold. This is reminiscent of the bacteriophage morphogenesis in which the sheath polymerizes on the tail tube [13,22].

Hcp1 modelling and validation

The EAEC Hcp1 protein was modelled based on the available Hcp three-dimensional crystal structures from *P. aeruginosa*, *E. tarda* and *Y. pestis* (PDB: 1Y12, 3HE1, 3EAA, 3V4H). The availability of multiple homologous structures offered the opportunity to build a robust multiple sequence alignment, improved and validated based on structural alignments.

To validate the EAEC Hcp1 model, we engineered the N115C variant, in which the asparagine residue at position 115 (Asn-115) is substituted by a cysteine. The Asn-115 residue is at the interface of two monomers within the hexamer, and is positioned to face the native cysteine residue (Cys-38) of the adjacent monomer (Fig 2A). The N115C Hcp1 mutant is functional as shown by its ability to be released in a T6SS-dependent manner (Supplementary Fig S3). Cells were treated with the oxidative agent copper phenanthroline, washed and free cysteines were blocked using N-ethylmaleimide (NEM) to avoid artifactual disulfide bond formation upon cell lysis. Analysis of cytoplasmic extracts from cells producing the N115C Hcp1 variant by non-reducing SDS-PAGE showed that Hcp1-N115C migrates as a ladder (Fig 2B), demonstrating formation of disulfide bridges between adjacent monomers. Overall these data validate the EAEC Hcp1 model and the experimental procedure. This model was further validated by the recently released structure of the Hcp1 protein [23].

Hcp1 hexamers assemble in a head-to-tail mode

To further evaluate the ability of Hcp1 to form tubular structures *in vivo* we reasoned that cysteine residues placed at the interface of two hexamers will form a disulfide bridge if Hcp hexamers polymerize. Our experiment approach draws its inspiration from the *in vitro* work of Ballister *et al* [12]. To identify the most probable interfaces between two Hcp hexamers, we modeled dodecamers in a head-to-tail, tail-to-tail or head-to-head orientation (Fig 3A-C). Interestingly, each of the available Hcp crystal structures describes a different, unique mode of interaction between Hcp hexameric rings: head-to-tail (*P. aeruginosa* Hcp1, [8]), tail-to-tail (*P. aeruginosa* Hcp3, [11]), and head-to-head (*E. tarda* EvpC, [10]). The three templates therefore offer bases for structural predictions regarding all possible stacking modes of EAEC Hcp1 hexamers. In each dodecamer model, the main contact is established by one loop on either side, yielding a limited choice of targets for cysteine substitutions (Fig 3A–C).

Cysteine substitutions were introduced into a cysteine-less (C38S) variant of the Hcp1 protein. For the head-to-tail assembly, cysteine residues were introduced at positions Gly96 (loop 4) and Ser158. Residues Gln24 (loop 1) and Ala95 (loop 4) were targeted for the tail-to-tail assembly, while residue Gly48 was mutated for the head-to-head assembly. All the Hcp1 variants accumulate at comparable levels and are functional as shown by their release in the extracellular milieu (Supplementary Fig S3).

SDS-PAGE analyses of cytoplasmic extracts from oxidized cells producing the variants showed that the G96C-S158C combination leads to the formation of a ladder corresponding to multiple oligomers, while the Q24C-A95C and G48C combinations remain monomeric (Fig 3D). These data support the hypotheses that (i) Hcp1 assembles into tubular structures *in vivo* and (ii) that the hexamers are stacked in a head-to-tail manner within the tube.

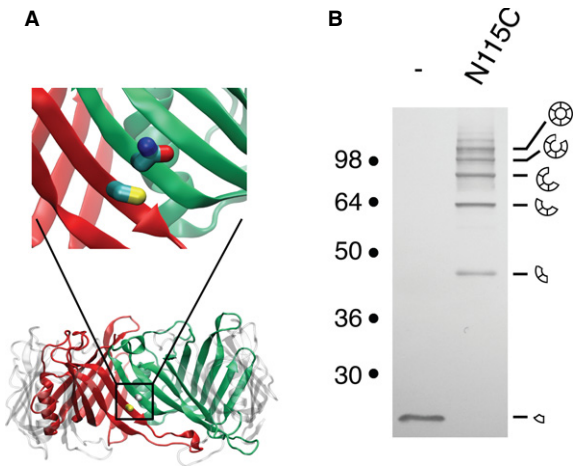

Figure 2. Lateral cross-linking validates the Hcp1 model.

A Model of the EAEC Hcp1 hexamer. Two adjacent monomers are colored in red and green, respectively. The magnification emphasizes the location of the Cys-38 (red monomer) and Asn-115 (green monomer) residues of the two adjacent monomers.

B Disulfide bond formation between Hcp1 proteins within the hexamer. Cytoplasmic extracts from EAEC Δ*hcp*1 cells producing Hcp1 or Hcp1-N115C after *in vivo* oxidative treatment were analyzed by 12.5%-acrylamide SDS-PAGE and proteins were immunodetected with the anti-FLAG monoclonal antibody. Positions of the Hcp1 monomer and oligomers are indicated on the right. Molecular weights (in kDa) are indicated on the left.

© 2014 The Authors

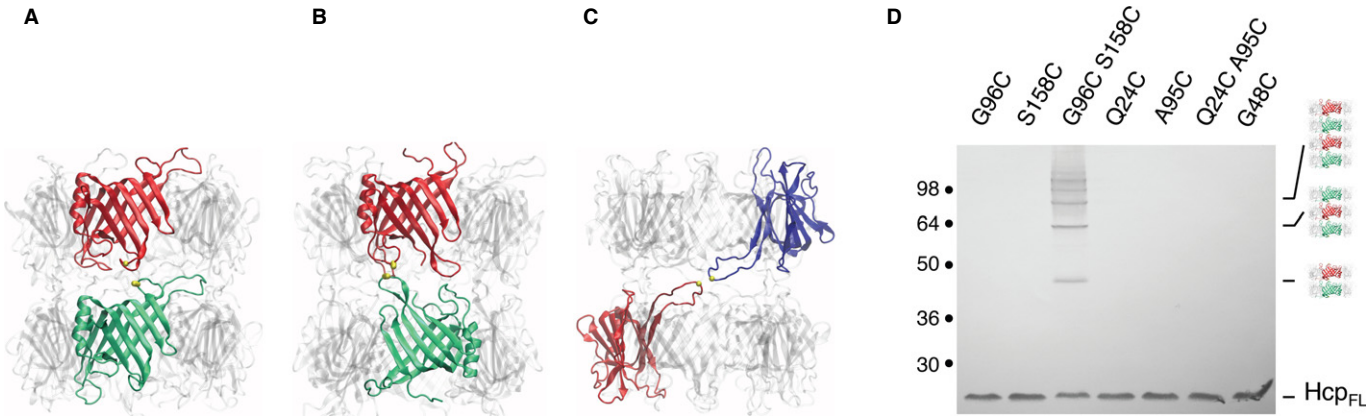

Figure 3. Hcp1 hexamers assemble tubular edifices by head-to-tail stacking *in vivo*.

A–C Models of EAEC Hcp1 hexamers assembled in a head-to-tail (A), tail-to-tail (B) or head-to-head (C) manner, based on the available crystal lattices. The locations of the cysteine substitutions used to probe the assembly are indicated by the yellow balls (Gly96 and Ser158 for the head-to-tail; Gln24 and Ala95 for the tail-to-tail; Gly48 for the head-to-head).

D Cytoplasmic extracts from EAEC Δ*hcp*1 cells producing the indicated Hcp1 C38S cysteine mutant proteins after *in vivo* oxidative treatment were analyzed by 12.5%-acrylamide SDS-PAGE and proteins were immunodetected with the anti-FLAG monoclonal antibody. Positions of the Hcp1 monomer and oligomers are indicated on the right. Molecular weights (in kDa) are indicated on the left.

To verify that hexamers are stacked in a head-to-tail manner, we engineered tryptophan variants with the rationale that insertion of a bulky tryptophan residue at the hexamer interface will destabilize the assembly of the tubular structure. Indeed, the Hcp1 S158W variant was not functional, as shown by Hcp release assay (Supplementary Fig S4). Identical results were obtained when residues located within the loop facing Ser138 (Asn93 and Gly96) were substituted by tryptophan residues (data not shown). Interestingly, fluorescence microscopy showed that production of the Hcp1 S158W protein prevents formation of dynamic TssB/C sheath structures (Fig 1D, *hcpW*$^+$), suggesting that Hcp hexamers polymerization into tubes is a prerequisite for T6SS sheath assembly.

Aberrant Hcp1 assembly in the cytoplasm of a *sci-1* T6SS-deficient strain

We then asked whether the assembly of the Hcp tube requires T6SS components. Formation of Hcp1 hexameric rings remains unaffected in the Δ*sci-1* strain (*i.e.*, which carries a deletion of the *sci-1* T6SS gene cluster; Fig 4A). However, all the cysteine combinations (G96C-S158C, Q24C-A95C and G48C) led to the formation of dimers or higher oligomeric forms, demonstrating that, in absence of any T6SS subunit, Hcp1 hexamers can pack in head-to-tail, tail-to-tail and head-to-head assemblies (Fig 4A). From these data we concluded that, while Hcp1 spontaneously forms hexameric rings, proper assembly of Hcp1 tubes *in vivo* is tightly controlled by Sci-1 T6SS components. During bacteriophage T4 biogenesis, a complex structure called the baseplate serves as a platform for tail tube/sheath polymerization and triggers sheath contraction as well [13]. The tube initiates its polymerization once the six wedges assemble onto the gp27-gp5 hub complex [13]. We therefore tested whether Hcp1 assembles tubular structures in absence of VgrG1, the T6SS homologue of the hub complex. As shown in Fig 4B, Hcp1 hexamers do not assemble in head-to-tail only in *vgrG1* cells, demonstrating that VgrG1 is required for proper assembly of Hcp1 tubes. However, VgrG1, when produced alone in the *Δsci-1* background, is not sufficient to restore the controlled Hcp1 assembly (Fig 4D). Finally, Hcp1 assembly is not impaired in *tssB1C1* cells (Fig 4E), a result consistent with phage morphogenesis as bacteriophage T4 sheath-less tails have been previously observed [22].

Conclusive remarks and outlook

The current models of Type VI secretion hypothesize that the Hcp proteins assemble into a structure resembling the bacteriophage tail tube [6]. Indeed, *in vitro* electron microscopy experiments showed that purified Hcp spontaneously assembles into small tubular edifices [6,11]. In contractile bacteriophages, the tail tube is surrounded by the sheath and serves as a scaffold during sheath polymerization [13,22]. In the T6SS, TssB and TssC form dynamic cytosolic structures resembling the phage sheath, providing further support to the assembly of similar contractile tail structures in both T6SS and bacteriophage T4 [14–17,20]. By analogy with the bacteriophage structure, the cytosolic portion of the T6SS is depicted as a sheath surrounding an Hcp tube. Here, we provide evidence that the EAEC Hcp1 protein interacts with the sheath-like TssB1/C1 complex through direct contacts with TssB1. Recently, an interaction between Hcp and both TssB and TssC has been reported in *Agrobacterium tumefaciens* [24]. In our bacterial two-hybrid and co-immunoprecipitation assays, we did not detect an interaction between Hcp1 and TssC1. Furthermore, we noted that Hcp1-TssB1 complex formation was of low affinity since chemical cross-linking was required to detect this interaction *in vivo*. This low affinity is compatible with a model in which the Hcp tube slides within the sheath during contraction. In agreement with the results obtained by Kapitein *et al* using immunofluorescence microscopy [15], the comparison of T6SS sheath assembly in WT and *hcp1* mutant strains using time-lapse fluorescence microscopy further showed that

 © 2014 The Authors

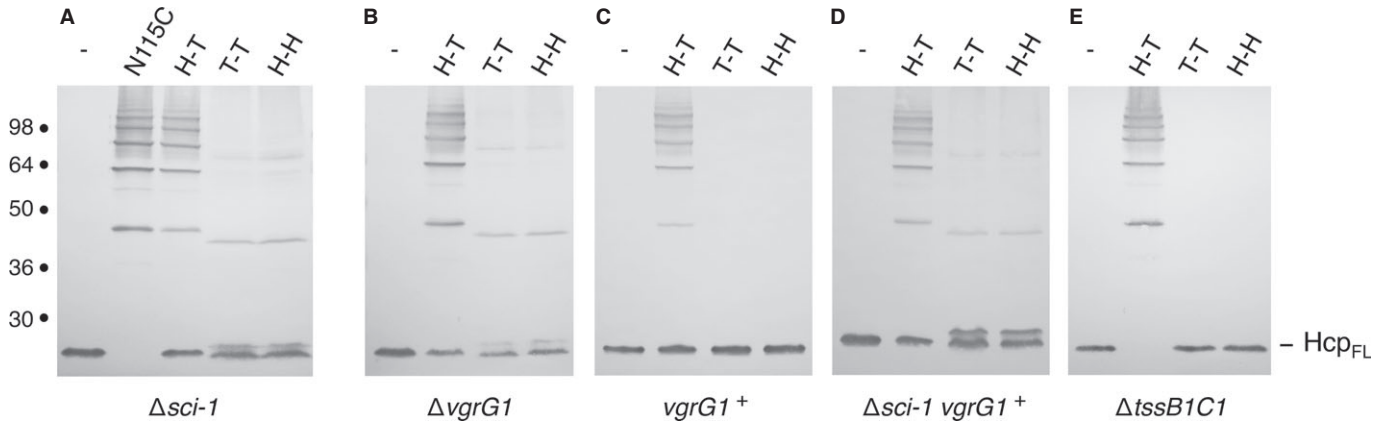

Figure 4. Proper assembly of Hcp1 tubes is a controlled phenomenon.

A–E Cytoplasmic extracts from EAEC Δ*sci-1* cells (A), Δ*vgrG1* (B), Δ*vgrG1* cells producing WT VgrG1 (*vgrG1*$^+$) (C), Δ*sci-1* cells producing WT VgrG1 (Δ*sci-1 vgrG1*$^+$) (D), or Δ*tssB1C1* cells (E) producing the cysteine-less Hcp1 variant (-) or Hcp1 variants to probe the lateral cross-linking (N115C), the head-to-tail (H-T; G96C-S158C), the tail-to-tail (T-T; Q24C-A95C), or the head-to-head (H-H; G48C) stacking modes were analyzed by 12.5%-acrylamide SDS-PAGE and proteins were immunodetected with the anti-FLAG monoclonal antibody. Position of the Hcp1 monomer is indicated on the right. Molecular weights (in kDa) are indicated on the left.

Hcp1 is required for sheath polymerization: in absence of Hcp1, TssB1-sfGFP dynamic structures were not observed and the fluorescence was diffuse. Additionally, we found that assembly of the sheath-like structure is dependent on Hcp1 tube formation as a tryptophan substitution disrupting Hcp1 tubular edifices prevents formation of the T6SS sheath. Although the mechanism by which T6SS sheath polymerization is dependent on Hcp has not been determined here, our data suggest that the TssB/C proteins assemble the sheath using the Hcp tube as a framework, as proposed during bacteriophage T4 tail morphogenesis [13,22].

The cysteine substitution approach revealed that Hcp1 assembles in an ordered manner *in vivo* in which hexameric rings stack head-to-tail onto one another. These results provide the first *in vivo* demonstration that Hcp subunits form a genuine tubular structure. While these novel data are key to a better understanding of the assembly mechanism of the T6SS, they also bring clues regarding phage structure. Indeed, due to the sheath density in cryo-electron microscopy images, the assembly mode of the tail tube of contractile phages has not been described yet [13]. However, the tail tube of the non-contractile bacteriophage λ is composed of 32 stacked hexamers of GpV [18]. Based on the data described here, and on the crystallographic observation that tailed bacteriophages and T6SS tubes are composed of similar building blocks [9], we propose that these tubes share a common organization. In the case of phages, the tail tube serves as a conduit for DNA and proteins delivery [13]. Interestingly, it was recently shown that protein toxins delivered by the T6SS can be loaded either onto the tip of the VgrG protein [7] or within the Hcp hexamer [25]. The formation of Hcp tubes therefore suggests that multiple toxins could be stored into the tube and delivered into the target cell by a single shot.

Importantly we show that proper assembly of the Hcp1 tube requires other T6SS subunits. Although the T6SS does not impact formation of the hexameric rings, implying that rings assemble spontaneously, one or several of the T6SS core components are required for proper polymerization of Hcp1 hexamers into tubes. We showed that while the TssB1 and TssC1 proteins are dispensable, VgrG1, the homologue of the gp27-gp5 hub, is required – but not sufficient – to promote proper Hcp1 assembly. Indeed, during phage tail biogenesis, tube and sheath polymerization is primed by the hub and the tail initiator complex and occurs once the baseplate has been completed. In the T6SS, the components of the baseplate are yet to be identified. The *in vivo* assay developed in this study may then be used to probe the different subunits of the T6SS and determine which subunit(s) control the ordered Hcp1 assembly. Among other exciting open questions, whether the Hcp tube length is regulated by a tape measure protein such as the bacteriophage T4 gp29 protein and whether dedicated chaperones are required for proper assembly of the Hcp tubes are now under investigation.

In sum, we showed that (i) Hcp form tubes of stacked hexamers, (ii) Hcp tube formation is required for sheath polymerization, (iii) TssB and TssC are not required for Hcp tube formation and (iv) VgrG is required for Hcp assembly. This is reminiscent of phage morphogenesis in which (i) formation of the tail tube initiates onto the central hub of the baseplate and (ii) the sheath is dispensable for tube assembly but use it as a template during polymerization. It is worth to note that subtle differences exist between T6SS tail assembly and bacteriophage tail morphogenesis such as the observations that phage tail tube proteins do not assemble as hexamers by their own or that phage tail tubes are extremely stable. However, the commonalities underlined by this study emphasize that the general mechanism underlying the assembly of these structures is likely conserved.

Materials and Methods

See Supplementary Materials and Methods for details of homology modeling, design of cysteine variants, fractionation, Hcp1 release, bacterial two-hybrid and co-immunoprecipitation procedures, and Supplementary Table S1 for list of strains, plasmids and oligonucleotides used in this study.

© 2014 The Authors

Bacterial strains, growth conditions and chemicals

Escherichia coli K12 DH5α was used for cloning procedures. The EAEC strain 17-2 and its Δ*sci-1*, Δ*hcp1*, Δ*vgrG1*, Δ*tssB1*, Δ*tssC1* and Δ*tssB1-C1* isogenic derivatives were used for this study. Strains were routinely grown in LB broth at 37°C, with aeration. Plasmids were maintained by the addition of ampicillin (100 μg/ml for K12, 200 μg/ml for EAEC) or chloramphenicol (40 μg/ml). Dichloro (1,10-phenanthroline) copper(II) (Cu-oP) and N-ethylmaleimide (NEM) were purchased from Sigma-Aldrich.

In vivo disulfide cross-linking

3×10^{10} exponential growing cells ($OD_{600} \sim 0.6$) were incubated with 0.3 mM Cu-oP for 20 min without agitation. Cells were then harvested by centrifugation and incubated in 10 mM HEPES (pH 7.4), Sucrose 30%, 1 mM EDTA and 2.5 mM NEM for 30 min on ice to block free thiol groups. Cells were pelleted by centrifugation and submitted to a fractionation procedure (see Supplementary Materials and Methods). Cytoplasmic extracts were mixed with loading buffer prior to analysis by SDS-PAGE and immunoblotting.

Time-lapse fluorescence microscopy

Overnight cultures of entero-aggregative *E. coli* 17-2 WT or mutant derivative strains carrying plasmid pBAD33-TssB1–sfGFP were diluted 1:100 into M9 minimal medium supplemented with glycerol (0.2%), vitamin B1 (1 μg/ml), casaminoacids (40 μg/ml), LB (10% v/v) and chloramphenicol 40 μg/ml. Cells were then cultivated for 6 hours to an $OD_{600nm} \sim 1.0$ in M9 minimal medium to maximize expression of the *sci-1* T6S gene cluster that is up-regulated in iron-depleted conditions [26]. Cells were washed in phosphate buffered saline (PBS), resuspended in PBS to an $OD_{600nm} \sim 50$ and spotted on a thin pad of 1.5% agarose in PBS and covered with a cover slip. Microscopy recordings have been performed as previously described [17].

Supplementary information for this article is available online: http://embor.embopress.org

Acknowledgments

We thank Tâm Mignot for fluorescence microscopy, Laure Journet, Petr Leiman (EPFL, Switzerland) and the members of the Cascales, Lloubès, Cambillau, Bouveret and Sturgis research groups for discussion, Oliver Uderso, Isabelle Bringer and Annick Brun for technical assistance, Patrick Vieira and Lionel Messing for plasmids. Work in the E.C. laboratory is supported by the Centre National de la Recherche Scientifique and a grant from the Agence Nationale de la Recherche (ANR-10-JCJC-1303-03). Y.R.B. was supported by a doctoral fellowship from the French Ministère de la Recherche.

Authors contributions

YRB, JH and EC designed and conceived the experiments; YRB, JH and EC provided tools; YRB, JH and HC performed the experiments; YRB, JH and EC wrote the article.

Conflict of interest

The authors declare that they have no conflict of interest.

References

1. Coulthurst SJ (2013) The Type VI secretion system - a widespread and versatile cell targeting system. *Res Microbiol* 164: 640 – 654
2. Silverman J, Brunet YR, Cascales E, Mougous JD (2012) Structure and regulation of the Type VI secretion system. *Annu Rev Microbiol* 66: 453 – 472
3. Cascales E, Cambillau C (2012) Structural biology of type VI secretion systems. *Philos Trans R Soc Lond B Biol Sci* 367: 1102 – 1111
4. Aschtgen MS, Gavioli M, Dessen A, Lloubes R, Cascales E (2010) The SciZ protein anchors the enteroaggregative *Escherichia coli* Type VI secretion system to the cell wall. *Mol Microbiol* 75: 886 – 899
5. Felisberto-Rodrigues C, Durand E, Aschtgen MS, Blangy S, Ortiz-Lombardia M, Douzi B, Cambillau C, Cascales E (2011) Towards a structural comprehension of bacterial Type VI secretion systems: characterization of the TssJ-TssM complex of an *Escherichia coli* pathovar. *PLoS Pathog* 7: e1002386
6. Leiman PG, Basler M, Ramagopal UA, Bonanno JB, Sauder JM, Pukatzki S, Burley SK, Almo SC, Mekalanos JJ (2009) Type VI secretion apparatus and phage tail-associated protein complexes share a common evolutionary origin. *Proc Natl Acad Sci USA* 106: 4154 – 4159
7. Shneider MM, Buth SA, Ho BT, Basler M, Mekalanos JJ, Leiman PG (2013) PAAR-repeat proteins sharpen and diversify the type VI secretion system spike. *Nature* 500: 350 – 353
8. Mougous JD, Cuff ME, Raunser S, Shen A, Zhou M, Gifford CA, Goodman AL, Joachimiak G, Ordonez CL, Lory S, Walz T, Joachimiak A, Mekalanos JJ (2006) A virulence locus of *Pseudomonas aeruginosa* encodes a protein secretion apparatus. *Science* 312: 1526 – 1530
9. Pell LG, Kanelis V, Donaldson LW, Howell PL, Davidson AR (2009) The phage lambda major tail protein structure reveals a common evolution for long-tailed phages and the type VI bacterial secretion system. *Proc Natl Acad Sci USA* 106: 4160 – 4165
10. Jobichen C, Chakraborty S, Li M, Zheng J, Joseph L, Mok YK, Leung KY, Sivaraman J (2010) Structural basis for the secretion of EvpC: a key type VI secretion system protein from *Edwardsiella tarda*. *PLoS One* 5: e12910
11. Osipiuk J, Xu X, Cui H, Savchenko A, Edwards M, Joachimiak A (2011) Crystal structure of secretory protein Hcp3 from *Pseudomonas aeruginosa*. *J Struct Funct Genomics* 12: 21 – 26
12. Ballister ER, Lai AH, Zuckermann RN, Cheng Y, Mougous JD (2008) *In vitro* self-assembly of tailorable nanotubes from a simple protein building block. *Proc Natl Acad Sci USA* 105: 3733 – 3738
13. Leiman PG, Arisaka F, van Raaij MJ, Kostyuchenko VA, Aksyuk AA, Kanamaru S, Rossmann MG (2010) Morphogenesis of the T4 tail and tail fibers. *Virol J* 7: 355
14. Basler M, Pilhofer M, Henderson GP, Jensen GJ, Mekalanos JJ (2012) Type VI secretion requires a dynamic contractile phage tail-like structure. *Nature* 483: 182 – 186
15. Kapitein N, Bönemann G, Pietrosiuk A, Seyffer F, Hausser I, Locker JK, Mogk A (2013) ClpV recycles VipA/VipB tubules and prevents non-productive tubule formation to ensure efficient Type VI protein secretion. *Mol Microbiol* 87: 1013 – 1028
16. Bönemann G, Pietrosiuk A, Diemand A, Zentgraf H, Mogk A (2009) Remodelling of VipA/VipB tubules by ClpV-mediated threading is crucial for type VI protein secretion. *EMBO J* 28: 315 – 325
17. Brunet YR, Espinosa L, Harchouni S, Mignot T, Cascales E (2013) Imaging Type VI secretion-mediated bacterial killing. *Cell Rep* 3: 36 – 41

 © 2014 The Authors

18. Davidson AR, Cardarelli L, Pell LG, Radford DR, Maxwell KL (2012) Long noncontractile tail machines of bacteriophages. *Adv Exp Med Biol* 726: 115 – 142
19. Boyer F, Fichant G, Berthod J, Vandenbrouck Y, Attree I (2009) Dissecting the bacterial type VI secretion system by a genome wide *in silico* analysis: what can be learned from available microbial genomic resources? *BMC Genomics* 10: 104
20. Zoued A, Durand E, Bebeacua C, Brunet YR, Douzi B, Cambillau C, Cascales E, Journet L (2013) TssK is a trimeric cytoplasmic protein interacting with components of both phage-like and membrane anchoring complexes of the type VI secretion system. *J Biol Chem* 288: 27031 – 27041
21. Zhang XY, Brunet YR, Logger L, Douzi B, Cambillau C, Journet L, Cascales E (2013) Dissection of the TssB-TssC interface during Type VI secretion sheath complex formation. *PLoS One* 8: e81074
22. King J (1968) Assembly of the tail of bacteriophage T4. *J Mol Biol* 32: 231 – 262
23. Douzi B, Spinelli S, Blangy S, Roussel A, Durand E, Brunet YR, Cascales E, Cambillau C (2014) Crystal structure and self-interaction of the Type VI secretion tail-tube protein from enteroaggregative *E. coli*. *PLoS One*, in press
24. Lin JS, Ma LS, Lai EM (2013) Systematic dissection of the *Agrobacterium* Type VI secretion system reveals machinery and secreted components for subcomplex formation. *PLoS One* 8: e67647
25. Silverman J, Agnello DM, Zheng H, Andrews BT, Li M, Catalano CE, Gonen T, Mougous JD (2013) Haemolysin coregulated protein is an exported receptor and chaperone for Type VI secretion substrates. *Mol Cell* 51: 584 – 593
26. Brunet YR, Bernard CS, Gavioli M, Lloubès R, Cascales E (2011) An epigenetic switch involving overlapping Fur and DNA methylation optimizes expression of a Type VI secretion gene cluster. *PLoS Genet* 7: e1002205

© 2014 The Authors